Journal of the Korean Vacuum Society
Vol. 4, No. 2, June 1995, pp. 194~200

〈 연구논문 〉

Microprobe EELS Study of Oxygen Non-Stoichiometry in High T_c $YBa_2Cu_3O_{7-\delta}$ Grain Boundaries

D. H. Shin and S. E. Babcock*

Department of Physics, Dongguk University, Seoul 100-715, Korea
**Department of Materials Science and Engineering, University of Wisconsin-Madison, USA*
(Received May 17, 1995)

전자에너지손실분광법(EELS)을 이용한 $YBa_2Cu_3O_{7-\delta}$ 고온초전도체 쌍결정 경계에서의 산소 조성변화 연구

신동혁 · S. E. Babcock*

동국대학교 물리학과
**Department of Materials Science and Engineering, University of Wisconsin-Madison, USA*
(1995년 5월 17일 접수)

요 약—2~3 nm의 공간분해능을 갖는 전자에너지손실분광법(Electron Energy Loss Spectroscopy, EELS)을 이용하여, 전기적 특성조사된 $YBa_2Cu_3O_{7-\delta}$ 고온초전도체 쌍결정의 결정경계(grain boundary)에서 산소의 조성변화를 조사하였다. Misorientation angle이 14°, 28°, 30°인 3개의 쌍결정 중에서 Josephson junction 특성을 보인 28°및 30°결정경계에서의 oxygen 1s absorption edge는 결정내부에서의 oxygen 1s absorption edge와 매우 다름을 알 수 있었다. 이는 결정경계에서의 산소조성이 결정내부에 비해 낮음을 의미하며, 그 영역이 결정경계 부근 20~40 nm로, coherence length에 비해 큼을 알 수 있다. 반면에, flux pinning 특성을 보인 14°결정경계에서의 oxygen 1s absorption edge는 결정내부에서와 별 차이를 보이지 않았다. 따라서 일반적으로 관찰되어온, misorientation angle이 큰 결정경계에서의 Josephson junction 특성은 결정경계 부근에서 산소의 조성이 낮아지는데에 기인하며, 그 원인은 결정경계면을 통해 산소가 out-diffusion되기 때문인 것으로 생각된다.

Abstract—The oxygen concentration at grain boundaries in electromagnetically-characterized, bulk-scale bicrystals of high T_c $YBa_2Cu_3O_{7-\delta}$ has been investigated using high-spatial resolution (2~3 nm) electron energy loss spectroscopy (EELS) in a TEM. Flux-grown bicrystals containing grain boundaries with misorientation relationships of 14°, 28°, and 30° about [001] have been studied. The 14° bicrystal showed flux-pinning (FP) critical current density characteristics, whereas the 28° and 30° bicrystals behaved like Josephson Junctions (JJ). The oxygen 1s absorption edge observed at the grain boundaries of Josephson junction bicrystals by TEM-EELS has a markedly different structure than those of the intragranular regions. The difference indicates a depressed charge carrier density and oxygen concentration in the boundary region. The carrier deficient zone extends from 20 to 40 nm into each crystal, a distance much larger than a coherence length in the direction perpendicular to the boundary. In striking contrast, the oxygen K-edges in spectra taken from the grain boundary with flux-pinning character are nearly identical to the intragranular spectra. The observed oxygen deficiency of the Josephson junction boundaries is consistent with a model in which the high-angle boundaries provide high-diffusivity paths for the oxygen diffusion out of the sample.

I. Introduction

The weak-link behavior observed for most high-angle grain boundaries in the high T_c $YBa_2Cu_3O_{7-\delta}$ superconductors is of central interest both for understanding the fundamental mechanism of their superconductivity and for their development for applications. Ironically, the discovery of this behavior's microstructural origin has proven to be one of the most challenging materials science problems posed by these materials.

Although exceptions have been found, high-angle boundaries ($\theta > 10^{\circ}$) usually are observed to act as weak links, whereas low-angle boundaries do not [1]. Several types of microstructural features have been identified as possible sources for this behavior. For example, the low-angle, high-angle distinction has suggested a role for primary grain boundary dislocations to many researchers. Thin layers of wetting second phase have been postulated and observed, as have thin regions of cation and oxygen non-stoichiometery. However, high-resolution transmission electron microscope (TEM) imaging and energy dispersive x-ray microanalysis (EDX) have suggested that the cation grain boundary core structure is narrower than a coherence length in the a-b plane, and that the cation non-stoichiometry is similarly restricted to a narrow boundary core, and not always present in Josephson-coupled boundaries [2-4]. Thus, a more general origin for weak link character most likely exists.

The obvious candidate for the observed weak-link character and its absence in a few special boundaries is the oxygen distribution in the vicinity of the boundary. The bulk scale electronic structure and superconducting properties are known to be sensitive to the oxygen stoichiometry and degree of order in the chain sites. Unfortunately, the subtle changes needed to produce large changes in the superconducting properties are extremely diffucult to detect with the high spatial resolution needed to understand the grain boundary properties. For example, high-resolution imaging is essentially insensitive to the position of the oxygen atoms. Furthermore, oxygen atoms can be removed from or added to the chain-sites with little change to the cation lattice, making high resolution imaging a less attractive tool for establishing correlations between observed microstructures and electromagnetic properties. The sensitivity of EDX to oxygen is sufficiently small to make it nearly impossible to achieve high-spatial resolution and sufficiently high precision under reasonable experimental conditions. The long counting times required almost always result in time-dependent desorption of the oxygen atoms.

On the other hand, electron energy loss spectroscopy (EELS) of the oxygen K-edge is very sensitive to changes in the electronic structure that are believed to correlate directly with the local oxygen concentration in $YBa_2Cu_3O_{7-\delta}$. High-quality spectra can be acquired in a few seconds, minimizing the changes of irradiation induced artifacts and providing a sensitive measure of local changes to the sample. Furthermore, unlike x-ray microanalysis, the spatial resolution of core-loss EELS is limited only by the electron probe size and stability of the electron microscope. In certain modern analytical microscopes, 2~3 nm resolution EELS microanalysis is routine [5, 6].

Zhu and coworkers recently have demonstrated the potential of EELS profiling of the grain boundary vicinity [7]. Their investigations of grain boundaries in polycrystalline materials provide two most interesting results. First, high-angle grain boundaries with full oxygen stoichiometry as well as grain boundaries of reduced oxygen content were discovered in the same samples. This result is consistent both with evidence for a percolative flux-pinning path in bulk sintered materials and with observations of a few special flux-pinning high-angle grain boundaries in bulk-scale and thin film boundaries. Second, they were able to explain which boundaries were oxygen deficient and which not on the basis of a constrained coincidence site lattice model.

However, they were unable to make the crucial step of characterizing the electrical properties of individual grain boundaries of oxygen deficiency and of full oxygen stoichiometry in order to establish a role for oxygen deficiency in controlling the grain boundary character.

In this paper, we describe oxygen-core loss EELS experiments conducted on three bicrystals of known electromagnetic character and microstructure at the subnanometer level. Two of the bicrystals showed the characteristics of Josephson coupling whereas the third was flux-pinning. Instead of the standard technique of quantitation using partial cross-section, we used the pre-edge peak in the oxygen 1s absorption spectra as a measure of the density of charge carrier holes near the fermi level. Although this technique is not quantitative, it has been shown that the pre-edge peak intensity is inversely proportional to δ in $YBa_2Cu_3O_{7-\delta}$, and comparisons can be made with spectra taken from samples of known oxygen concentration.

II. Experiments

The $YBa_2Cu_3O_{7-\delta}$ bicrystals used for this study were grown by a flux technique [8]. They generally contain two rectangular-plate-shaped grains whose [001] axes are aligned within 1° and whose [100] (or [010]) axes are rotated relative to one another by the misorientation angle θ. Three high-angle bicrystals with known electromagnetic properties were chosen for the TEM-EELS experiments. Their misorientation angles are 14°, 28°, and 30°. Their electromagnetic properties are described in the next paragraph. Over a substantial fraction of their length, the grain boundaries in these samples appeared to thread the thin dimension of the bicrystal (along [001]), resulting in a large fraction of nearly tilt-type boundary area. Pure tilt boundary facets lie perpendicular to the high-conductivity a-b planes of the structure, thus allowing for electrical transport across the boundary in a long-coherence length direction.

The macroscopic superconducting properties of the three bicrystals were measured prior to thinning for TEM. Features of their resistivity vs. temperature characteristics and of the dependence of their transport critical current density (J_c) on magnetic field at both low (mT) and high (up to 7 T) applied field were studied to determine if each bicrystal's J_c was limited by a flux-pinning or a Josephson junction mechanism. Both the 28° sample and the 30° sample acted like Josephson junctions [9]. The 14° sample showed flux-pinning characteristics. This result was somewhat unexpected because 14° is a large θ value in the context of earlier measurments [10]. It is also intriguing, because flux-pinning character has been observed previously in a different bicrystal with essentially this same misorientation relationship.

The bicrystals were polished mechanically and ion-milled to make TEM specimens. Care was taken to minimize the surface damage during ion-milling by cooling the sample nearly to liquid nitrogen temperature and choosing a low ion accellerating-voltage (~3 kV), a low ion-current, and a low beam-incidence angle. Nevertheless, thin amorphous layers inevitably formed on the surfaces. Since, in our experience, this amorphous $YBa_2Cu_3O_{7-\delta}$ is oxygen-deficient, its existence was considered during the experimentation and in the analysis of the spectra. The 28° and 30° bicyrstals both had been thinned for TEM approximately one year prior to EELS experimentation. Within two weeks of the experiment, the 30° bicrystal was reoxygenated by annealing for 15 minutes at 350 ℃ in flowing high-purity oxygen. According to Rothman's oxygen diffusion data, this heat treatment results in a diffusion distance greater than 100 nm, assuring that the sample was fully oxygenated in the thin, electron transparent region [11]. A short, low-voltage (2.5 kV) ion-milling step was needed to produce good thin area subsequent to the oxygen anneal. The 14° sample had been oxygenated and characterized within 4 weeks prior to ion thinning, and

viewed by TEM-EELS within a few days.

Prior to EELS experimentation, structure images of the grain boundary region of each sample were obtained. As with previous Josephson junction and flux-pinning samples, the boundaries appeared free of grain boundary second phases. Furthermore, the cation structural width of the grain boundary appeared to be less than ~0.5 nm, a value of typical oxide materials. No other obvious microstructural defects were observed to wet the boundary region.

The EELS experiments were carried out on a Hitachi HF2000 high resolution analytical TEM equipped with a Gatan model 666 Parallel-detection Electron Energy Loss Spectrometer (PEELS). A cold field-emission source and a double condenser lens system produce an electron probe about 2 nm in diameter. Thus, the spatial resolution of the experiment is 2~3 nm.

A relatively low electron accelerating voltage (100 keV) was used for spectroscopy because the threshhold for the knock-on damage to $YBa_2Cu_3O_{7-\delta}$ structure is ~150 keV [12]. Irradiation-induced changes in the oxygen K-edge shape were noticeable at 200 kV over periods comparable with the spectrum acquisition times used here (~30 seconds total). As noted by previous authors, the intensity of the pre-edge peak decreased with exposure to the electron beam, indicating a loss of oxygen from the sample [13, 14] No noticeable changes were observed in the spectrum for exposures of at least several minutes with the 100 keV electron probe used to acquire the data presented below. A liquid nitrogen-cooled stage was used to prevent contamination of the irradiated area. Liquid-nitrogen cooling also appears to reduce the irradiation-induced oxygen depletion rate.

EEL spectra were acquired in diffraction mode with a spectrometer entrance aperture diameter of 3 mm. Because the beam was incident along the *c*-axis of both crystals, ambiguities due to the crystal orientation dependence of the spectra are avoided. Profiles of the boundary region were obtained by beginning at the grain boundary and advancing into the grain on either side. Thus, artifactual evidence of oxygen depletion due to electron irradiation was avoided. All spectra from each sample were obtained at approximately the same thicknesses by moving the probe parallel to the edge of the TEM sample. The spectra were acquired using the Gatan EL/P software at a dispersion of 0.1 eV per channel. For each location on the sample, ten spectra, each of three seconds acquisition time, were collected in sequence. These spectra were inspected for time dependent changes, and then added together when none were found. Thus, a total of ~10^4 counts per channel was acheived. To correct for spectrometer drift, the energies in each acquired spectrum were shifted arbitrarily to position the main K-edge peak at ~538 eV. Background subtraction was performed by non-linear least squares fitting to the standard $A_o \exp(-r)$ function.

III. Results

Fig. 1 shows the variation in the oxygen 1s absorption edge shape as a function of distance from the grain boundary in the 28° bicrystal. The grain boundary spectrum is markedly different from the in-grain spectrum not only in that it lacks the pre-edge peak at 528 eV, but also its main peak is broadened by a few eV. A small shoulder appears in the pre-edge structure about 10 nm from the boundary core. Approximately 40 nm away it reaches a level which is only slightly weaker than that at 100 nm. Because the pre-edge peak does not increase further beyond 100 nm, the spectrum at 100 nm may be considered as representative of the intragranular region. The profile taken into the opposite grain showed all of the same features as that shown in Fig. 1.

Similar results have been obtained from the 30° Josephson junction boundary (Fig. 2). As observed in the 28° sample (Fig. 1), evidence for an extended region of oxygen deficiency is apparent in the profile of pre-edge structure *vs.* distance from the boundary. The fine structures of the

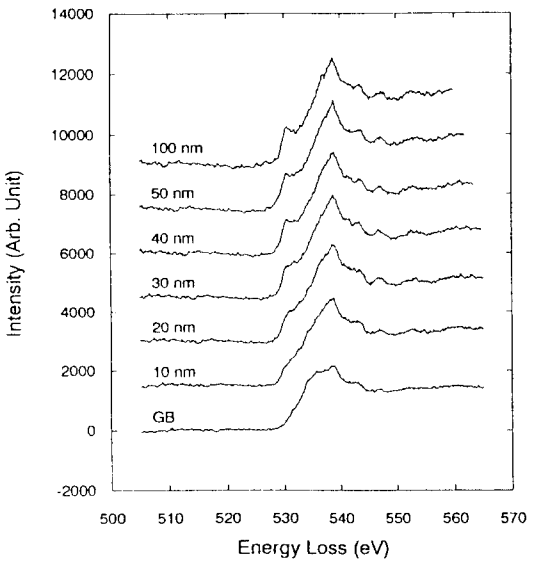

Fig. 1. The variation in the EELS oxygen 1s absorption edge shape as a function of distance from the grain boundary in the 28° Josephson junction bicrystal. An extended region of oxygen deficiency is apparent in the profile of pre-edge structure *vs.* distance from the boundary.

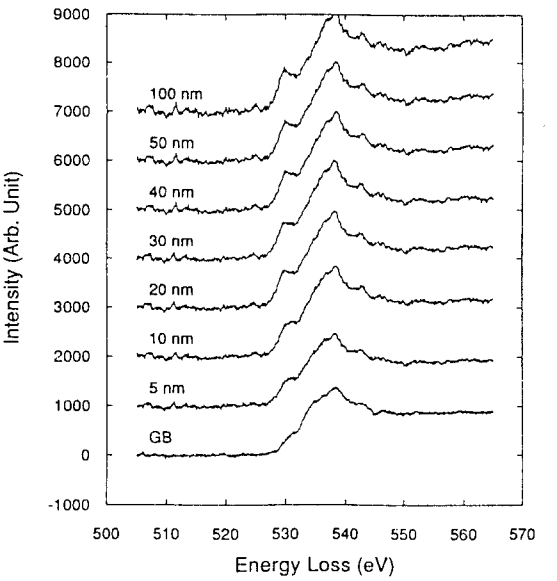

Fig. 2. The variation in the EELS oxygen 1s absorption edge shape as a function of distance from the grain boundary in the 30° Josephson junction bicrystal. Similar to the 28° boundary, evidence for an extended region of oxygen deficiency is apparent in the profile of pre-edge structure *vs.* distance from the boundary.

spectra including two small peaks above the main peak are reproduced in Fig. 1 and Fig. 2. However, this grain boundary shows a pre-edge shoulder at its core, indicating that it may be slightly less oxygen-deficient than the 28° boundary is. The width of the oxygen-deficient region also appears narrower for the 30° specimen. For example, the spectrum collected 20 nm from the 30° boundary is comparable to that collected 40 nm from the 28° boundary. We concede that more measurements must be taken on a variety of samples and at several positions along each grain boundary to establish a variability of the core width. However, the important observation here is that the key features of the spectral profile are the same for both Josephson junction boundaries.

Fig. 3 contains EEL spectra obtained from the 14° specimen prepared from the sample with flux-pinning J_c characteristics. The profile is clearly distinguishable from those of the 28° and 30° specimens in that no changes in the pre-edge structure are apparent right up to the boundary core. The 528 eV pre-edge peak at the grain boundary is just as strong as the intragranular spectrum and remains roughly the same throughout. The variation that just precedes the pre-edge peak in the GB spectrum is an artifact of the channel-to-channel gain variation in the spectrometer. Its 5 eV shift with distance from the boundary core is an indication of the spectrometer drift rate during the experimentation.

IV. Discussion

The spectra collected here can be compared with those of Browning *et al.*, recorded on samples of "known" oxygen concentration, to estimate the local value of δ in the grain boundary region and the magnitude of the oxygen deficiency at the grain boundary [14]. Such comparisons indicate that the spectra in Fig. 1 represent a change of oxygen concentration from

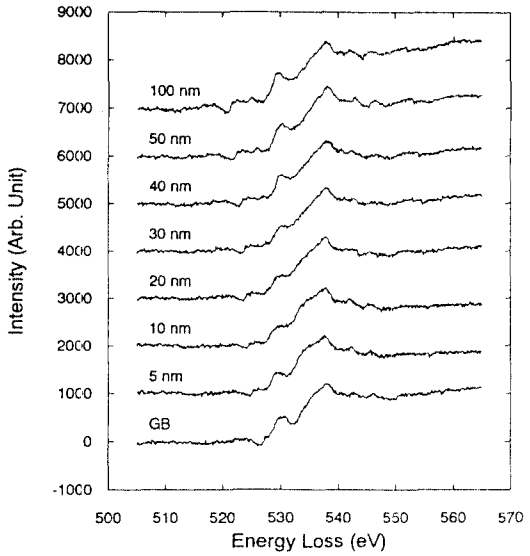

Fig. 3. EEL spectra obtained from the 14° specimen prepared from the sample with flux-pinning J_c characteristics. The shapes of the oxygen 1s absorption edge are nearly same in all the spectra indicating that the oxygen concentaration is uniform.

~6.8 in the intragranular regions to ~6.0 at the grain boundary core. The bulk-scale electromagnetic properties of the bicrystals (*e.g.*, T_c ~ 94 K) suggest that the measured oxygen concentrations are too low. The fact that the in-grain spectra do not have stronger pre-edge peak reprsentative of a fully-oxygenated sample may be due to the experimental conditions used here. There is an oxygen-deficient amorphous layer on the surface of the TEM sample produced during ion-milling. The acquired spectrum is an average from the whole thickness.

The oxygen deficiencies at the grain boundaries of the 28° and 30° samples may be the origin of their bulk-scale Josephson junction behavior. Such deficiencies will cause the grain boundary regions to become a lower T_c superconductor at the regions near the grain boundary core, and, perhaps, insulating right at the core, resulting in the formation of SS′S- or SS′IS′S-type Josephson junction. A uniform oxygen concentration observed in the 14° flux-pinning boundary is also consistent with its electromagnetic character and with this interpretation of the role of oxygen deficiency.

The changes of the pre-edge peaks in Josephson junction boundaries, although not quantitative, suggest resemblance with the diffusion profile which would be obtained in a sample when the surface concentration is maintained constant. This may be the case for the bicrystal if the grain boundaries are a diffusion path for the oxygen atoms in the direction normal to the surface. Due to the low diffusivity, oxygen atoms cannot easily move in the direction of *c*-axis inside the grains. On the other hand, the diffusivity is much larger in the *a-b* plane. If a diffusion path along *c*-direction is present, oxygen atoms will diffuse in the *a-b* plane to the grain boundaries where they can diffuse out of the sample. Using the diffusivity data of Rothman *et al.* [11], the diffusion lengths of several hundred angstroms in the *a-b* plane is obtained using $(Dt)^{1/2}$ at room temperature for diffusion time of one year. Thus the difference in the widths of the oxygen deficient regions in the two samples may be due to the fact that one sample was recently re-oxygenated while the other one was not.

The oxygen concentration profile in a fresh, bulk bicrystal grain boundaries may not be the same as those in the thin TEM samples. However, if the diffusion model is valid, the Josephson junction boundaries in bulk bicrystals will still be oxygen deficient although the oxygen deficient region may be narrower. In fact, a narrower oxygen deficient region may be more appropriate to explain the Josephson junction behavior in the high T_c superconductors. Note that the electromagnetic properties of the samples were characterized before thinning for TEM, and that the effect of diffusion will become more prominent in the TEM samples due to the fact that their thicknesses are comparable to the room temperature diffusion length of the oxygen atoms in the *a-b* planes.

V. Conclusion

In conclusion, we have observed that high-angle (001)-tilt boundaries in $YBa_2Cu_3O_{7-\delta}$ bicrystals with Josephson junction character are oxygen deficient. This oxygen deficiency may be the origin of their weak-link character. The oxygen deficiency may be caused by out-diffusion of oxygen through the grain boundaries. In contrast, oxygen concentration is nearly uniform in flux-pinning boundaries, in consistence with their larger, field-independent J_c values.

Acknowledgement

The authors are grateful to the collaborators at Cornell University, University of Wisconsin-Madison, and Northwestern University. The present studies were supported in part by the Basic Science Research Program, Ministry of Education, 1991 Project No. BSRI-'94-2443.

References

1. S. E. Russek, D. K. Lathrop, B. H. Moeckly, R. A. Buhrman, D. H. Shin and J. Silcox, Appl. Phys. Lett. **57**, 1155 (1990).
2. D. H. Shin, J. Silcox, S. E. Russek, D. K. Lathrop, B. Moeckly and R. A. Buhrman, Appl. Phys. Lett. **57**, 508 (1990).
3. S. E. Babcock, X. Y. Cai, D. C. Larbalestier and D. L. Kaiser, Nature **347**, 167 (1990).
4. S. E. Babcock, MRS Bulletin **17**, 20 (1992).
5. A. Ando, K. Saiki, K. Ueno and A. Koma, Japan. J. Appl. Phys. **27**, L304 (1988).
6. R. F. Egerton, *Electron Energy Loss Spectroscopy in the Electron Microscope* (Plenum Press, New York, 1986).
7. Y. Zhu, H. Zhang, H. Wang and M. Suenaga, J. Mater. Res. **6**, 2507 (1991).
8. D. L. Kaiser, F. Holtzberg, B. A. Scott and T. R. McGuire, Appl. Phys. Lett. **51**, 1040 (1987).
9. D. C. Larbalestier, S. E. Babcock, X. Y. Cai, M. B. Field, Y. Gao, N. F. Heinig, D. L. Kaiser, K. Merkle, L. K. Williams, N. Zhang, Physica C **185**, 315 (1991).
10. D. Dimos, P. Chaudhari, J. Mannhart and F. K. LeGoues, Phys. Rev. Lett. **61**, 219 (1988).
11. S. J. Rothman, J. L. Routbort and J. E. Baker, Phys. Rev. B **40**, 8852 (1989).
12. M. A. Kirk, M. C. Baker, J. Z. Liu and D. J. Lam, Mat. Res. Soc. Symp. Proc. **99**, 209 (1988).
13. D. H. Shin, PhD Thesis, Cornell University (1991).
14. N. D. Browning, J. Yuan and L. M. Brown, Supercond. Sci. Technol. **4**, 346 (1991).